American Mineralogist, Volume 83, pages 947–951, 1998

Calculated role of aluminum in the incorporation of ferric iron into magnesium silicate perovskite

NICOLA C. RICHMOND,* AND JOHN P. BRODHOLT

Research School of Geological and Geophysical Sciences, Birkbeck College and University College, Gower Street, London WC1E 6BT, U.K.

ABSTRACT

An atomistic computer simulation study was undertaken to address the role of Al in the substitution of ferric iron into magnesium silicate perovskite, $MgSiO_3$. Calculated substitution and vacancy energies at 0 K were used to consider two different substitution mechanisms: (a) Fe^{3+} and Al independently charge balanced by vacancies or by a similar cation in another site, or (b) Fe^{3+} and Al charge balancing each other. Our results show that it is preferential by 1 to 2 eV for Fe^{3+} to substitute into an Mg site charge balanced by an Al substitution into an Si site. This is increasingly favorable if the Fe^{3+} and Al substitute into adjacent sites. The coupled substitution occurs because it is energetically unfavorable for Al to enter the dodecahedral site.

INTRODUCTION

Magnesium silicate perovskite and magnesiowüstite are considered to be the dominant phases in the Earth's lower mantle, and as a result were subjects of much experimental and theoretical work. Of these two phases, experimental evidence had indicated that the Fe in the lower mantle preferentially occupies sites in magnesiowüstite (Katsura and Ito 1996, and others). However, this result has come into question following recent experiments on more realistic lower mantle assemblages containing a few weight percent Al_2O_3. Irifune (1994) reported high pressure (up to 28 GPa) phase changes in a pyrolite mantle, indicating that Al_2O_3 is mainly accommodated in $MgSiO_3$ with small amounts accepted into $CaSiO_3$, with no creation of an aluminous phase. The experiments of Wood and Rubie (1996) on mixtures containing up to 4.1 wt% Al_2O_3 indicated that the presence of Al causes a significant shift in the partitioning ratio of Fe between perovskite and magnesiowüstite with approximately equal amounts of Fe in each phase. McCammon (1997) also reported an increase in Fe concentration in perovskite samples containing 3.3 wt% Al_2O_3. The presence of Al also tends to increase the proportion of Fe^{3+} in perovskite (Lauterbach et al. 1997). These results could have significant repercussions on our understanding of the dynamics of the lower mantle and transport properties such as electrical conductivity. In this study, an atomistic computer simulation technique was used to investigate the energies associated with Fe^{3+} and Al substitutions into the Mg or Si sites of orthorhombic magnesium silicate perovskite. The following sections outline the method used and summarize the structural results. These are then used to determine the energies associated with different substitution mechanisms, leading to a discussion of the possible role of Al in the substitution of Fe^{3+} into perovskite.

METHOD

Ideally, ab initio methods should be used to determine optimum structures and substitution energies, however, such methods are limited to a small number of atoms due to the computationally intensive nature of the codes. The technique used in this study, therefore, is an atomistic method based on the Born model of the atom. The PARAPOCS code (Parker and Price 1989) was used, enabling the study of cells containing up to 360 atoms.

Interatomic forces were modeled using Buckingham potentials, combining the Born-Mayer form of the repulsive energy and the r^{-6} dispersive interaction. Parameters (Table 1) were taken from Lewis and Catlow (1985), with the exception of the Si-O potential and the three-body interactions that were taken from Sanders et al. (1984) and the Al-O potential from Catlow et al. (1982). These potentials were applied successfully to past studies of high pressure silicates (for example, Price et al. 1989 and Wright and Price 1989), whereas the Al-O potential was developed by fitting to α-Al_2O_3 experimental data and was successfully applied to a study of defect energies in α-Al_2O_3 (Catlow et al. 1982). Charges on the O species of 0.84819 eV (core) and −2.84819 eV (shell) were used. This model was selected because it successfully modeled polarization, which, although important in addressing the energetics of defect formation, is not represented by all potential models (for example, Matsui 1996). The Lewis and Catlow (1985) parameters in Table 1 are based originally on the study of binary oxides and assume fully ionic charges. Ab initio calculations on $MgSiO_3$ (Cohen et al. 1989) revealed little evidence of covalent bonding, with the more accurate quantum mechanical approach

* E-mail: n.richmond@ucl.ac.uk

0003–004X/98/0910–0947$05.00

TABLE 1. Buckingham potential parameters used for perfect lattice and defect calculations

Cation	Charge	A (eV)	ρ (Å)
Mg	2	1428.5	0.2945
Al	3	1474.4	0.3006
Fe	3	1102.4	0.3299
Si	4	1283.9	0.3205

Note: From Lewis and Catlow (1985) except the Al potential (from Catlow et al. 1992) and the Si potential (from Sanders et al. 1984). Potential cutoff = 12 Å, harmonic core-shell interaction on O (k^s) = 74.92, constant in three-body force, O-Si-O, (k^b) = 2.09.

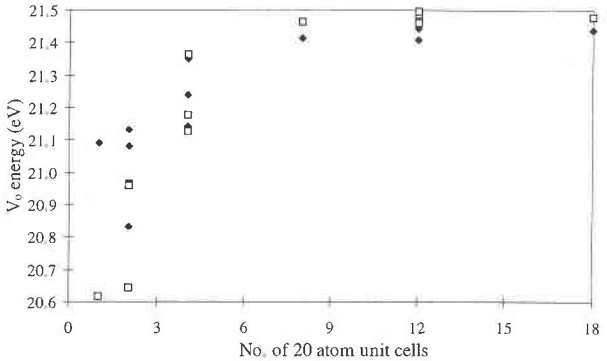

FIGURE 1. Convergence of defect energy with increasing cell size for an O vacancy. Multiple points for a specific number of unit cells correspond to different dimensions, for example, four cells could be arranged as 2 × 2 × 1, 2 × 1 × 2, or 1 × 2 × 2. Filled diamonds = apex. Open squares = equatorial.

showing good agreement with simpler atomistic models. Further, because we consider only isolated substitutions of Fe^{3+}, the issue of electron delocalization identified in the presence of Fe^{2+} and Fe^{3+} in perovskite (Fei et al. 1994) is not a factor here, and thus an ionic potential for Fe^{3+} is appropriate. Similarly, ab initio studies on vacancies in forsterite using pseudopotentials and the generalized gradient approximation gave good agreement with calculations performed using empirical pair potentials (Brodholt 1997), as have studies on defects in MgO using empirical and quantum mechanical methods (Grimes et al. 1989). The good agreement shown between ab initio and pair-potential methods indicates that the use of ionic potentials is justified.

It was necessary to use the same potential parameters for substitutions of Fe or Al regardless of whether they are introduced into the Mg site (dodecahedral) or the Si site (octahedral). Both potentials were fit originally to results from octahedral sites but, due to limited data on Fe or Al in dodecahedrally coordinated sites, potentials fit to that specific case are not available. The use of the same potential parameters enables direct comparison of energies, for example, Fe^{3+} introduced into the Mg or Si site, and it is believed that the inaccuracies created by the choice of parameters are minor relative to the results obtained.

Perfect lattice calculations were carried out for the phases of interest at 0 and 100 GPa. The minimum lattice energies and calculated cell parameters (Table 2) show good agreement with previous studies using the same potential model (for example, Price et al. 1989 and Wright and Price 1993) and results from studies using a quantum mechanical approach (D'Arco et al. 1993). Reasonable agreement (Table 2) was attained with experimentally determined data, where available. The 100 GPa perovskite results show a tetragonal structure, but these are 0 K results and thus do not consider thermal vibrations. Consequently, this indicated structural change is not reliable and we used the orthorhombic structure here. We have used hematite (α-Fe_2O_3) as the source of the Fe^{3+} and Al (with Al treated as defects occupying Fe^{3+} sites in the structure). It is stressed, however, that the different substitution mechanisms considered are for reactions involving equal numbers of Fe^{3+} and Al atoms. In this way, all comparisons we make are independent of the Fe^{3+} and Al source, and consequently applicable regardless of the actual lower mantle source. Similarly, equal amounts of

TABLE 2. Minimum lattice energies (LE) and cell parameters

Lattice	Pressure (GPa)	LE (eV)	Calculated cell parameters			Experimental cell parameters		
			a (Å)	b (Å)	c (Å)	a (Å)	b (Å)	c (Å)
$MgSiO_3$	0	−169.87	4.824	4.846	6.843	4.778*	4.933*	6.901*
$MgSiO_3$	100	−167.94	4.513	4.513	6.418	4.402†	4.548†	6.359†
MgO	0	−41.31	4.198	4.198	4.198	4.212‡	4.212‡	4.212‡
MgO	100	−40.26	3.859	3.859	3.859	3.822§	3.822§	3.822§
SiO_2	0	−129.07	3.965	3.965	2.843	4.180‖	4.180‖	2.667‖
SiO_2	100	−128.03	3.611	3.611	2.841			
Fe_2O_3	0	−149.46	5.127	5.162	13.397	5.036#	5.036#	13.749#
Fe_2O_3	100	−146.94	4.778	4.713	10.592			

Note: An orthorhombic structure was used for $MgSiO_3$; cubic for MgO; rutile structure SiO_2; corundum structure for Fe_2O_3.
References for experimental data are:
* Ross and Hazen (1990) for P = 0.01 GPa.
† Knittle and Jeanloz (1987) for ~102–112 GPa and 12% Fe.
‡ Deer et al. (1992).
§ Mao and Bell (1979) at 94.1 GPa.
‖ Ross et al. (1990) at 0.0001 GPa.
Nat. Bur. Standards Monograph 25 (1981).

TABLE 3. Substitution and vacancy energies in $MgSiO_3$

Type of substitution		Vacancy energies (eV) at 0 GPa	at 100 GPa
Single vacancies	$\square_{Si}''''$	94.37	97.17
	$\square_{Mg}''$	25.00	24.36
	$\square_{O}^{\bullet\bullet}$	21.49	20.22
Si/Mg substitutions	$Si_{Mg}^{\bullet\bullet}$	−64.10	−66.01
	Mg_{Si}''	68.82	74.40
Fe^{3+} substitutions	$Fe_{Mg}^{\bullet}$	−22.88	−22.57
	Fe_{Si}'	44.03	47.84
Al substitutions	$Al_{Mg}^{\bullet}$	−27.07	−28.38
	Al_{Si}'	38.92	41.07
Combined substitutions	$Fe_{Mg}^{\bullet}$ and Al_{Si}'	15.76	18.09
	$Al_{Mg}^{\bullet}$ and Fe_{Si}'	16.72	19.10

MgO and SiO_2 are generated for each substitution mechanism of interest, and consequently any errors in calculating the lattice energies for these do not affect the overall result.

Defect calculations were carried out keeping the lattice cell parameters fixed at the optimized values. Individual defects were introduced into the structure and the atomic positions then relaxed until a minimum energy was obtained. Defects were introduced into cells containing from 20 to 360 atoms, with the associated defect energy seen to converge with increasing cell size. This effect is due to the removal of the distortion of the structure due to the introduction of a defect into a small cell and to the removal of defect-defect interactions between adjacent cells. Typically for perovskite, the energy converged for a cell containing 240 atoms and an example of this convergence is shown in Figure 1 for an O vacancy.

RESULTS

Substitution energies of Fe^{3+} and Al into the Mg and Si sites of $MgSiO_3$ perovskite were determined together with the energy associated with Si, Mg, and O vacancies in pure magnesium perovskite and Mg substituting for Si and vice versa. The results in Table 3 use the standard Kröger and Vink (1956) notation, except that □ denotes a single vacancy. The single vacancy energies obtained for Si and Mg sites are approximately half of the site energies presented by Smyth and Bish (1987), indicating the importance of relaxation of the structure around the defect site.

These results (Table 3) agree with the 0 GPa vacancy results of Wall and Price (1989) and the Fe substitution and vacancy calculations of Wright and Price (1989). The 100 GPa results show significant differences from the 60 GPa values of Wright and Price (1989), but this discrepancy is believed to be related to problems with the code used in that study (K. Wright 1997, personal communications).

In addition, the energy associated with the substitution of Al into Fe_2O_3 was determined for the pressures of interest. For 0 GPa, a value of −3.99 eV was obtained and −4.81 eV at 100 GPa. These values are needed to determine the energy associated with different substitution mechanisms, but as discussed previously, the conclusions are independent of this Al and Fe_2O_3.

The question we wish to address is what role Al plays in the incorporation of Fe^{3+} in perovskite. This role can be determined by looking at two different methods of substituting Al and Fe^{3+}. In one method, the species substitute independently with the Al or Fe^{3+} charge balanced by vacancies or by a similar cation in another lattice site.

TABLE 4. Substitution mechanisms considered for Fe^{3+} and Al with associated energies

Label	Mechanism	Energy (eV) at 0 GPa	at 100 GPa
A	$Fe_2O_3 + 3Mg_{Mg}^{x} \rightarrow 2Fe_{Mg}^{\bullet} + \square_{Mg}'' + 3MgO$	4.77	5.37
B	$2Fe_2O_3 + 4Mg_{Mg}^{x} + Si_{Si}^{x} \rightarrow 4Fe_{Mg}^{\bullet} + \square_{Si}'''' + 4MgO + SiO_2$	3.73	5.84
C	$Fe_2O_3 + 3Mg_{Mg}^{x} + Si_{Si}^{x} \rightarrow 2Fe_{Mg}^{\bullet} + Si_{Mg}^{\bullet\bullet} + \square_{Si}'''' + 3MgO$	10.04	12.17
D	$Fe_2O_3 + 2Mg_{Mg}^{x} + Si_{Si}^{x} \rightarrow 2Fe_{Mg}^{\bullet} + Mg_{Si}'' + MgO + SiO_2$	2.14	7.91
E	$Fe_2O_3 + Mg_{Mg}^{x} + Si_{Si}^{x} \rightarrow Fe_{Mg}^{\bullet} + Fe_{Si}' + MgO + SiO_2$	0.23	3.92
F	$Fe_2O_3 + Mg_{Mg}^{x} + 2Si_{Si}^{x} + 2O_{O}^{x} \rightarrow 2Fe_{Si}' + \square_{Mg}'' + \square_{O}^{\bullet\bullet} + MgO + 2SiO_2$	6.05	11.10
G	$Fe_2O_3 + 3Si_{Si}^{x} + 3O_{O}^{x} \rightarrow 2Fe_{Si}' + \square_{Si}'''' + 3V_{O}^{\bullet\bullet} + 3SiO_2$	9.17	16.37
H	$Fe_2O_3 + 2Si_{Si}^{x} + O_{O}^{x} \rightarrow 2Fe_{Si}' + \square_{O}^{\bullet\bullet} + 2SiO_2$	0.87	6.79
I	$Fe_2O_3 + Mg_{Mg}^{x} + 2Si_{Si}^{x} \rightarrow 2Fe_{Si}' + Si_{Mg}^{\bullet\bullet} + MgO + SiO_2$	3.04	8.32
J	$Fe_2O_3 + Mg_{Mg}^{x} + 3Si_{Si}^{x} + 3O_{O} \rightarrow 2Fe_{Si}' + Mg_{Si}'' + \square_{Mg}'' + 3\square_{O}^{\bullet\bullet} + 3SiO_2$	8.60	17.96
K	$(Al,Fe)_2O_3 + 3Mg_{Mg}^{x} \rightarrow 2Al_{Mg}^{\bullet} + \square_{Mg}'' + 3MgO$	4.37	3.37
L	$2(Al,Fe)_2O_3 + 4Mg_{Mg}^{x} + Si_{Si} \rightarrow 4Al_{Mg}^{\bullet} + \square_{Si}'''' + 4MgO + SiO_2$	3.33	3.84
M	$(Al,Fe)_2O_3 + 3Mg_{Mg}^{x} + Si_{Si}^{x} \rightarrow 2Al_{Mg}^{\bullet} + Si_{Mg}^{\bullet\bullet} + \square_{Si}'''' + 3MgO$	9.64	10.17
N	$(Al,Fe)_2O_3 + 2Mg_{Mg}^{x} + Si_{Si}^{x} \rightarrow 2Al_{Mg}^{\bullet} + Mg_{Si}'' + MgO + SiO_2$	1.74	5.91
O	$(Al,Fe)_2O_3 + Mg_{Mg}^{x} + 2Si_{Si}^{x} + 2O_{O} \rightarrow 2Al_{Si}' + \square_{Mg}'' + \square_{O}^{\bullet\bullet} + MgO + 2SiO_2$	3.81	7.18
P	$(Al,Fe)_2O_3 + 3Si_{Si}^{x} + 3O_{O} \rightarrow 2Al_{Si}' + \square_{Si}'''' + 3\square_{O}^{\bullet\bullet} + 3SiO_2$	6.91	12.45
Q	$(Al,Fe)_2O_3 + 2Si_{Si}^{x} + O_{O}^{x} \rightarrow 2Al_{Si}' + \square_{O}^{\bullet\bullet} + 2SiO_2$	−1.37	2.87
R	$(Al,Fe)_2O_3 + Mg_{Mg}^{x} + 2Si_{Si}^{x} \rightarrow 2Al_{Si}' + Si_{Mg}^{\bullet\bullet} + MgO + SiO_2$	0.80	4.40
S	$(Al,Fe)_2O_3 + Mg_{Mg}^{x} + 3Si_{Si}^{x} + 3O_{O} \rightarrow 2Al_{Si}' + Mg_{Si}'' + \square_{Mg}'' + 3\square_{O}^{\bullet\bullet} + 3SiO_2$	6.36	14.04
T	$(Al,Fe)_2O_3 + Mg_{Mg}^{x} + Si_{Si}^{x} \rightarrow Al_{Mg}^{\bullet} + Al_{Si}' + MgO + SiO_2$	−1.09	0.96

Note: Reactions A to J involve substitutions of $2Fe^{3+}$. K to T involve 2Al. For reaction B and L the presented energies are half the values determined for the full equation, this corresponds to the substitution of two atoms, enabling direct comparison with the other reactions.

TABLE 5. Coupled substitution mechanisms considered for Fe^{3+} and Al with associated energies (in eV) at 0 and 100 GPa

Label	Mechanism	Energy (eV) at 0 GPa	Energy (eV) at 100 GPa
U	$2(Al,Fe)_2O_3 + Mg^{\times}_{Mg} + 3Si^{\times}_{Si} + O^{\times}_{O} \rightarrow Fe^{\bullet}_{Mg} + Fe'_{Si} + 2Al'_{Si} + \square''_{O} + MgO + 3SiO_2$	−1.14	—
V	$2(Al,Fe)_2O_3 + 2Mg^{\times}_{Mg} + 2Si^{\times}_{Si} \rightarrow Fe^{\bullet}_{Mg} + Fe'_{Si} + Al^{\bullet}_{Mg} + Al'_{Si} + 2MgO + 2SiO_2$	—	4.88
W	$2(Al,Fe)_2O_3 + 2Mg^{\times}_{Mg} + 2Si^{\times}_{Si} \rightarrow 2Fe^{\bullet}_{Mg} + 2Al'_{Si} + 2MgO + 2SiO_2$	−1.78	3.92
X	$2(Al,Fe)_2O_3 + 2Mg^{\times}_{Mg} + 2Si^{\times}_{Si} \rightarrow 2(Fe^{\bullet}_{Mg}, Al'_{Si}) + 2MgO + 2SiO_2$	−2.34	3.10
Y	$2(Al,Fe)_2O_3 + 2Mg^{\times}_{Mg} + 2Si^{\times}_{Si} \rightarrow 2Al^{\bullet}_{Mg} + 2Fe'_{Si} + 2MgO + 2SiO_2$	0.06	5.84

Note: For 0 GPa the minimum energy independent substitution was for one Fe^{3+} in each site and two Al in the Si site balanced by vacancies (reactions E and R in Table 4). At 100 GPa the minimum energies were obtained from one Fe^{3+} in each site and one Al in each site (reactions E and O in Table 4). The notation $(Fe^{\bullet}_{Mg}, Al'_{Si})$ refers to the adjacent substitution of the species.

The second option is that the Fe and Al directly charge balance each other, one in the Mg site and the other in the Si site. For this mechanism, the species could substitute into random sites, or into directly adjacent sites, with the associated energy possibly different for each. The lowest energy mechanism will be the most favorable, and thus it can be seen if direct charge balancing of Fe^{3+} and Al is more energetically favorable then the separate substitution of the species.

Four main substitutions were considered for Fe^{3+} or Al into the Mg or Si sites. The possible substitution mechanisms considered are presented in Table 4, together with the associated energies at 0 and 100 GPa. For completeness, all possible methods involving Si, Mg, and O vacancies and substitutions of Mg for Si and vice versa were considered, even though many are extremely unfavorable due to the creation of many vacancies.

At both 0 and 100 GPa, the most favorable method for incorporating two Fe^{3+} atoms is by reaction E, where the Fe^{3+} substitute into both the cation and Si site thereby directly charge balancing each other and creating no vacancies. Similar reactions can be considered for the substitution of two Al atoms (Table 4). In contrast to the substitution of Fe^{3+}, at 0 GPa it is favorable by 0.28 eV for both Al's to substitute into the Si site charge balanced by O vacancies (reaction R). This indicates that the substitution of Al into the dodecahedral site is highly unfavorable at low pressures. However, at 100 GPa the most favorable mechanism is for the Al to substitute into the Si and cation site, directly charge balancing each other with no vacancies created (O). This is similar to the best method for incorporating Fe^{3+}. Data obtained at 30 GPa for reactions R and O indicate that O is most favorable at this pressure, suggesting that over the range of mantle pressures, the most energetically favorable Al substitution is for Al simultaneously entering both sites.

Last, we compare these results for independent substitution mechanisms of Fe^{3+} and Al into perovskite (Table 4), with mechanisms where Fe^{3+} and Al directly charge balance each other. These results (Table 5) correspond to the energies of incorporation of two Fe^{3+} and two Al into the structure.

The lowest energy mechanisms are those where Al is restricted to the Si site and Fe to the dodecahedral site (W and X). Any mechanism with Al in the dodecahedral site is less favorable (V and Y). The most favorable mechanism is X where the Al and Fe occupy adjacent sites, although even if they are isolated (W) it is still significantly more favorable than when Al is in the divalent cation site. We conclude, therefore, that the reason the partitioning of Fe^{3+} increases strongly in perovskite when Al is present is simply that the substitution of Al into the divalent cation site is energetically unfavorable, with between 1 and 2 eV of energy saved by charge balancing the Al with Fe^{3+} in the dodecahedral site. These results are all obtained for 0 K, but preliminary high-temperature calculations at 2000 K and 100 GPa indicate that mechanism X remains most favorable by 1.0 eV. Consequently, it is believed that the results presented here are applicable to lower mantle conditions. Further, it is noted that experimental evidence has suggested that electron delocalization between Fe^{2+} and Fe^{3+} may play a role in stabilizing Fe^{3+} in perovskite (Fei et al. 1994). Our calculations demonstrate that Al in the mantle tends to encourage the substitution of Fe^{3+} in perovskite and this, combined with the stabilizing role of electron delocalization, will tend to increase the favorability of Fe^{3+} incorporation into perovskite in the mantle. We further note that studies of point defect equilibrium concentrations (Hirsch and Shankland 1991) have highlighted the abundance of specific defects over different thermodynamic conditions and the corresponding preferred substitutions of Fe^{3+} based on defect calculations performed by Wall and Price (1989), Wright and Price (1989) and others. The results presented here indicate that, in such models, the presence of Al must be considered as it favors the introduction of Fe^{3+} into the Mg site.

Finally, we stress that reactions V, W, X, and Y all use the same amount of product and reactant phases $(Al,Fe)_2O_3$, MgO, and SiO_2. This means that the results do not depend on (a) how accurately the energies of these phases are calculated, or (b) what these phases are. The product could just have been $MgSiO_3$ and the reactant could have been some other Al phase.

ACKNOWLEDGMENTS

We thank David Price and Atul Patel for their help and advice, and Catherine McCammon and an anonymous reviewer for useful comments. Nicola Richmond acknowledges the receipt of a NERC studentship, and

J.P.B. is grateful to the Royal Society for a University Research Fellowship.

References cited

D'Arco, P., Sandrone, G., Dovesi, R., Orlando, R., and Saunders, V.R. (1993) A quantum mechanical study of the perovskite structure type of $MgSiO_3$. Physics and Chemistry of Minerals, 20, 407–414.

Brodholt, J. (1997) Ab initio calculations on point defects in forsterite (Mg_2SiO_4) and implications for diffusion and creep. American Mineralogist, 82, 1049–1053.

Catlow, C.R.A., James, R., Mackrodt, W.C., and Stewart, R.F. (1982) Defect energetics in α-Al_2O_3 and rutile TiO_2. Physical Review B, 25, 1006–1026.

Cohen, R.E., Boyer, L.L., Mehl, M.J., and Pickett, W.E. (1989) Electronic structure and total energy calculations for oxide perovskites and superconductors. In A. Navrotsky and D.J. Weidner, Eds., Perovskite: A Structure of Great Interest to Geophysics and Material Science, 146 p. American Geophysical Union, Washington, D.C.

Deer, W.A., Howie, R.A., and Zussman, J. (1992) An introduction to the rock-forming minerals 2nd edition, 696 p. Longman Scientific and Technical, Harlow, U.K.

Fei, F., Virgo, D., Mysen, B.O., Wang, Y., and Mao, H.K. (1994) Temperature-dependent electron delocalization in (Mg,Fe)SiO_3 perovskite. American Mineralogist, 79, 826–837.

Grimes, R.W., Catlow, C.R.A., and Stoneham, A.M. (1989) A comparison of defect energies in MgO using Mott-Littleton and quantum mechanical procedures. Journal of Physics: Condensed Matter, 1, 7367–7384.

Hirsch, L.M. and Shankland, T.J. (1991) Point defects in (Mg,Fe)SiO_3 perovskite. Geophysical Research Letters, 18, 1305–1308.

Irifune, T. (1994) Absence of an aluminous phase in the upper part of the Earth's lower mantle. Nature, 370, 131–133.

Katsura, T. and Ito, E. (1996) Determination of Fe-Mg partitioning between perovskite and magnesiowüstite. Geophysical Research Letters, 23, 2005–2008.

Knittle, E. and Jeanloz, R. (1987) Synthesis and equation of state of (Mg,Fe)SiO_3 perovskite to over 100 Gigapascals. Science, 235, 668–670.

Kröger, F.A. and Vink, H.H. (1956) Relations between the concentrations of imperfections in crystalline solids. In F. Seitz and D. Turnbull, Eds., Solid State Physics, p. 307–435. Academic Press, New York.

Lauterbach, S., McCammon, C.A., and Seifert, F. (1997) Effects of alumina on Fe^{3+} content in perovskites under lower mantle conditions. Berichte der Deutschen Mineralogischen Gesellschalf. Beiheft zur European Journal of Mineralogy, 9(1), 219.

Lewis, G.V. and Catlow, C.R.A. (1985) Potential models for ionic oxides. Journal of Physics C: Solid State Physics, 18, 1149–1161.

Mao, H.-K. and Bell, P.M. (1979) Equation of state of MgO and ϵ-Fe under static pressure conditions. Journal of Geophysical Research, 84, 4533–4536.

Matsui, M. (1996) Molecular dynamics study of the structures and bulk moduli of crystals in the system CaO-MgO-Al_2O_3-SiO_2. Physics and Chemistry of Minerals, 23, 345–353.

McCammon, C. (1997) Perovskite as a possible sink for Ferric iron in the lower mantle. Nature, 387, 694–696.

Parker, S.C. and Price, G.D. (1989) Computer modelling of phase transitions in minerals. Advances in Solid State Chemistry, 1, 295–327.

Price, G.D., Wall, A., and Parker, S.C. (1989) The properties and behaviour of mantle minerals: a computer simulation approach. Philosophical Transactions of the Royal Society of London, A328, 391–407.

Ross, N.L. and Hazen, R.M. (1990) High-pressure crystal chemistry of $MgSiO_3$ perovskite. Physics and Chemistry of Minerals, 17, 228–237.

Ross, N.L., Shu, J.-F., Hazen R.M., and Gasparik, T. (1990) High-pressure crystal chemistry of stishovite. American Mineralogist, 75, 739–747.

Sanders, M.J., Leslie, M., and Catlow, C.R.A. (1984) Interatomic potentials for SiO_2. Journal of the Chemical Society, Chemical Communications, 1271–1274.

Smyth, J.R. and Bish, D.L. (1987) Crystal structures and cation sites of the rock-forming minerals, p. 311–319. Allen and Unwin, London, U.K.

Wall, A. and Price, G.D. (1989) Defects and diffusion in $MgSiO_3$ perovskite: a computer simulation. In A. Navrotsky and D.J. Weidner, Eds., Perovskite: A Structure of Great Interest to Geophysics and Material Science, 146 p. American Geophysical Union, Washington, D.C.

Wood, B.J. and Rubie, D.C. (1996) The effect of alumina on phase transformations at the 660-kilometer discontinuity from Fe-Mg partitioning experiments. Science, 273, 1522–1524.

Wright, K. and Price, G.D. (1989) Computer simulation of Fe in magnesium silicate perovskite. Geophysical Research Letters, 16, 1399–1402.

———(1993) Computer simulation of defects and diffusion in perovskites. Journal of Geophysical Research, 98, B12, 22245–22253.

Manuscript received February 2, 1998
Manuscript accepted May 5, 1998
Paper handled by Lars Stixrude